

Transmission Electron Microscopy Study of the Heavy-Ion-Irradiation-Induced Changes in the Nanostructure of Oxide Dispersion Strengthened Steels

S. V. Rogozhkin^{a, b, *}, A. A. Bogachev^{a, b}, N. N. Orlov^{a, b}, O. A. Korchuganova^{a, b}, A. A. Nikitin^{a, b},
A. G. Zaluzhnyi^{a, b}, M. A. Kozodaev^{a, b}, T. V. Kulevoy^a, R. P. Kuibeda^a, P. A. Fedin^a, B. B. Chalykh^a,
R. Lindau^c, Ya. Hoffman^c, A. Möslang^c, P. Vladimirov^c, and M. Klimenkov^c

^a*Institute for Theoretical and Experimental Physics named by A.I. Alikhanov of National Research Centre “Kurchatov Institute,”
Moscow, 117218 Russia*

^b*National Research Nuclear University MEPhI (Moscow Engineering Physics Institute), Moscow, 115409 Russia*

^c*Karlsruhe Institute of Technology, Karlsruhe, Germany*

**e-mail: Sergey.Rogozhkin@itep.ru*

Received December 1, 2016

Abstract—Transmission electron microscopy was used to study the effect of heavy-ion irradiation on the structure and the phase state of three oxide dispersion strengthened (ODS) steels: ODS Eurofer, ODS 13.5Cr, and ODS 13.5Cr–0.3Ti (wt %). Samples were irradiated with iron and titanium ions to fluences of 10^{15} and $\sim 3 \times 10^{15} \text{ cm}^{-2}$ at 300, 573, and 773 K. The study of the region of maximum radiation damage shows that irradiation increases the number density of oxide particles in all samples. The fraction of fine inclusions increases in the particle size distribution. This effect is most pronounced in the ODS 13.5Cr steel irradiated with titanium ions at 300 K to a fluence of $3 \times 10^{15} \text{ cm}^{-2}$. It is demonstrated that oxide inclusions in ODS 13.5Cr–0.3Ti and ODS 13.5Cr steels are more stable upon irradiation at 573 and 773 K than upon irradiation at 300 K.

Keywords: ODS (oxide dispersion strengthened) steels, nanostructure, irradiation, heavy ions, oxides, transmission electron microscopy

DOI: 10.1134/S0036029517070126

INTRODUCTION

Oxide dispersion strengthened (ODS) steels have been developed as structural materials for advanced fission and fusion reactors [11]. Modern ODS steels contain a great number of nanosized oxide inclusions, most of which are yttrium oxides, providing perfect operational properties of materials at elevated temperatures (for example, high-temperature creep resistance) [2, 3]. The atom-probe tomography studies of ODS steels have revealed a large number of nanoclusters enriched in a number of elements (Y, O, V, Ti, etc.).

The decisive role in the radiation stability of ODS steels belongs to the stability of their strengthening nanostructures. The earlier studies of the radiation effect on the ODS Eurofer steel revealed the exchange of chemical elements between nanoclusters and the matrix [4–6] and obtained data indicating the dissolution of oxide particles during low-temperature (600 K) irradiation [4].

This work is devoted to study of the effect of heavy-ion irradiation on the structure evolution of ODS steels, namely, ODS 13.5Cr, ODS 13.5Cr–0.3Ti (wt %), and ODS Eurofer by transmission electron microscopy. The changes in nanosized oxide inclusions after irradiation with 100-keV/nucleon Fe^{2+} and Ti^{2+} ions to fluences of $\sim 10^{15}$ and $\sim 3 \times 10^{15} \text{ cm}^{-2}$ at 300, 573 and 773 K were investigated.

EXPERIMENTAL

Initial Materials

The following steels were analyzed: high-chromium model steels¹ Fe–13.5Cr–0.3Y₂O₃ and Fe–13.5Cr–0.3Ti–0.3Y₂O₃ [7] and ODS Eurofer steel [3]. These materials were produced by mechanical alloying of the powders of initial base steel, yttrium oxide, and titanium (in the case of alloy with addition of tita-

¹ Hereinafter, ODS 13.5Cr and ODS 13.5Cr–0.3Ti steels.

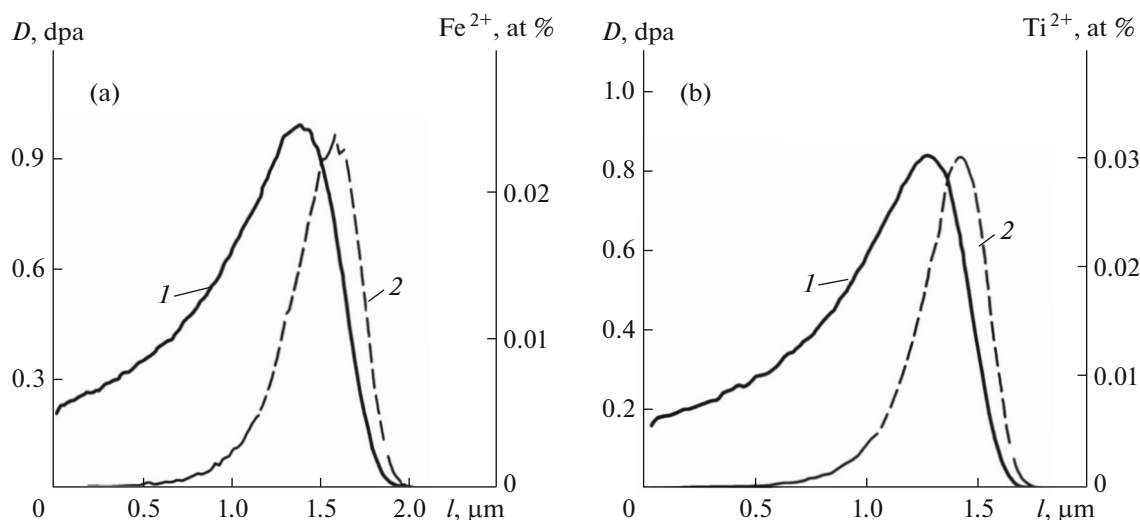


Fig. 1. Radiation damage profiles calculated using the SRIM program ((1) $D(l)$ is the damaging dose) and the ion implantation profiles ((2) change in the fraction of penetrated ions X^{2+}) in iron specimen for Fe^{2+} ions (a) with energy of 5.6 MeV and for Ti^{2+} ions (b) with energy of 4.8 MeV. The calculations were made for a fluence of 10^{15} cm^{-2} .

nium) in an attritor mill. The powders of the charge materials were placed into steel capsules for degassing, pressing, electron-beam welding of the capsule cap, and compacting. The ODS Eurofer and ODS 13.5Cr steels were produced using hot isostatic pressure (HIP) at a pressure of 100 MPa and temperatures of 1150 and 1100°C, respectively. The ODS 13.5Cr–0.3Ti steel was compacted by hot extrusion at 1100°C. The ODS Eurofer steel was additionally heat-treated under the following conditions: annealing at 980°C for 30 min and tempering at 760°C for 2 h. The high-chromium ODS steels were not subjected to heat treatment.

Irradiation Experiment

The effect of heavy-ion irradiation on the stability of the nanostructure of the ODS steels was investigated using transmission electron microscopy (TEM). The materials under study were irradiated on a TIPr-1 accelerator (heavy-ion prototype) by 100-keV/nucleon Fe^{+2} and Ti^{2+} ions (5.6 and 4.8 MeV, respectively) [8, 9]. The calculations carried out using the SRIM computer simulation tool showed that the region where the number of radiation-induced defects is maximum located at a depth l of 1.4 and 1.25 μm , respectively, from the irradiated sample surface (Fig. 1). The Kinchin–Pease model [10] was used for calculating the equivalent irradiation dose (dpa). ODS steel samples were irradiated to fluences of 1×10^{15} and $3 \times 10^{15} \text{ ion/cm}^2$ at 300, 573, and 773 K.

Sample Preparation

Disk-shaped samples were 3 mm in diameter. The samples were mechanically thinned to a thickness of 100 μm . The surface roughness of the samples was controlled using atomic force microscopy before and after irradiation. The roughness was less than 50 nm.

The samples were mechanically polished with a SiC paper and electrochemically thinned in a 20% solution of sulfuric acid and methanol at 18°C using Tenupol-5 equipment for subsequent TEM examination. The initial and irradiated ODS steel samples were examined by TEM in an FEI Tecnai F20 and JEOL JEM 1200EX transmission electron microscopes, and the latter was equipped with an LaB_6 cathode.

The samples taken from the region with the maximum damaging dose were prepared for TEM in two stages. At the first stage, a layer $1.3 \pm 0.1 \mu\text{m}$ thick was electrochemically removed from the irradiated surface. At the second stage, the samples were thinned from the nonirradiated side.

RESULTS AND DISCUSSION

Examination of the Initial State

The data for quantitative comparison of the TEM results obtained for initial states of the steels are listed in Table 1. A microstructure analysis of the initial states of the materials shows a bimodal grain size distribution for the high-chromium ODS steels (Fig. 2) [7, 11]. The steel without titanium exhibits single nanosized grains inside coarse grains $\sim 6\text{--}8 \mu\text{m}$ in size, the ODS 13.5Cr–0.3Ti steel contains agglomerates of

Table 1. TEM quantitative analysis of the microstructure features of the initial state of the ODS Eurofer and ODS 13.5Cr–(0–0.3)Ti steels using a FEI Tecnai F20 microscope

Characteristic	ODS Eurofer	ODS 13.5Cr	ODS 13.5Cr–0.3Ti
Grain size, μm : ferrite	4–7	6–8	6–8
martensite	–	0.4–0.8	0.1–0.7
Carbide size, nm	50–800	–	–
Oxides:			
average size \bar{d}_{ODS} , nm	11 ± 6	10 ± 3	5 ± 2
number density N_{ods} , m^{-3}	5×10^{21}	8×10^{21}	3×10^{22}
Dislocation density, m^{-3}	$\sim 10^{14}$	$\sim 10^{14}$	$\sim 10^{14}$

100–700-nm grains, and the ODS Eurofer steel includes coarse ferrite grains with size of $\sim 4\text{--}7\ \mu\text{m}$.

In the materials under study, the precipitation of coarse particles along grain boundaries were observed: up to 100 nm in ODS 13.5Cr(0–0.3)Ti and $>200\text{nm}$ in ODS Eurofer. The analysis of electron diffraction patterns of ODS Eurofer which were selected in the areas including those particles showed that they are $M_{23}\text{C}_6$ carbides [12]. In the ODS 13.5Cr–(0–0.3)Ti steel, coarse inclusions are yttrium or yttrium-titanium oxides [7].

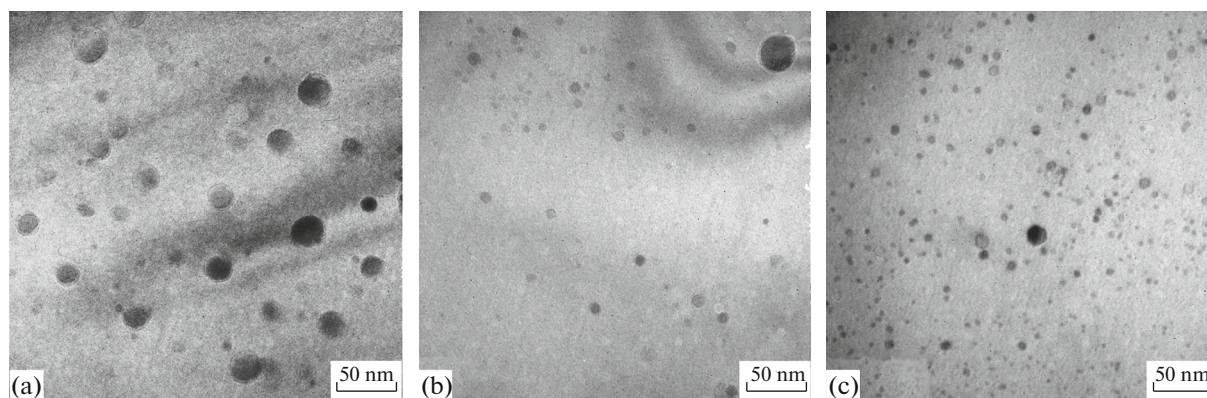
The high-chromium ODS steels exhibit a nonuniform spatial distribution of particles in the shape of liner structures. These structures could be formed during HIP of a material and they seem to be located along edge dislocations or at the boundaries of the former grains. TEM dark-field images suggest a large number of nanosized inclusions that possess the same

orientation within a grain and have the structure of oxides. According to [7, 13], the stoichiometry of these particles are Y_2O_3 and $\text{Y}_2\text{Ti}_2\text{O}_7$, in the case of high-chromium alloys.

Figures 3 and 4 demonstrate oxide particle size (d_{ODS}) distribution histograms. The average size and the number density of oxide inclusions are given in Table 1. The addition of titanium to the steel (ODS 13.5Cr–0.3Ti) significantly reduced the average size and increased the number density of oxide inclusions in the material.

Examination of the Irradiated State

An analysis of the material microstructure after irradiation with heavy ions showed the shape and size stability of the grains at all temperatures. Irradiation increases the number density of interstitial dislocation

**Fig. 2.** Typical bright-field images of the microstructure in steels (a) ODS Eurofer, (b) ODS 13.5Cr, and (c) ODS 13.5Cr–0.3Ti in the initial state.

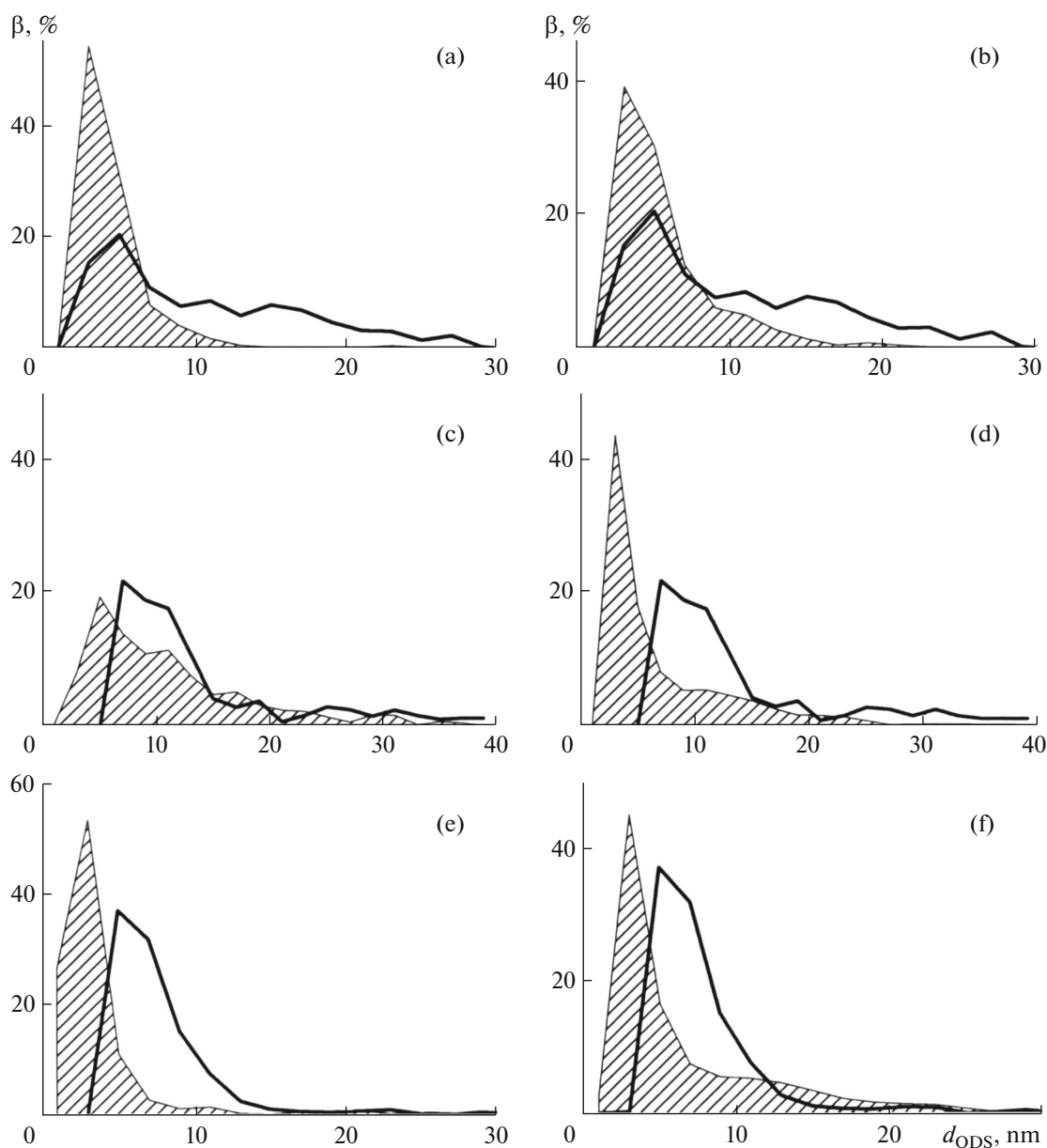


Fig. 3. Oxide particle size (d_{ODS}) distribution histograms (β is the fraction of particles) in steels (a, b) ODS Eurofer, (c, d) ODS 13.5Cr, and (e, f) ODS 13.5Cr–0.3Ti in the initial state (solid thick lines) and after irradiation (thin lines) by (a, c, e) Fe^{2+} and (b, d, f) Ti^{2+} ions at 300 K to a fluence of 10^{15} cm^{-2} .

loops in all samples. The density of loops in the material volume with a high density of oxide particles after irradiation was $\sim 10^{14} \text{ m}^{-2}$, and it was $\sim 10^{16} \text{ m}^{-2}$ in the material volume with a low density of inclusions. The observed effect confirms [14] that oxide particles play the role of recombination centers and tend to reduce the density of survived radiation-induced defects in the region with a high density of oxides. Table 2 lists the results of a quantitative analysis of oxide inclusions in all irradiated samples.

The ion irradiation reduced the average size and increased the number density of oxide inclusions in all samples. The most pronounced effect was observed for the ODS 13.5Cr steel irradiated by titanium ions up to a dose of 2.4 dpa at 300 K. Figures 3 and 4 demonstrate the change in the size distribution of oxide particles in the ODS steels. The irradiation by titanium and iron ions up to a dose of 0.8 dpa at 300 K leads to a shift in the size distribution of the observed inclusions toward small sizes. This effect was also observed

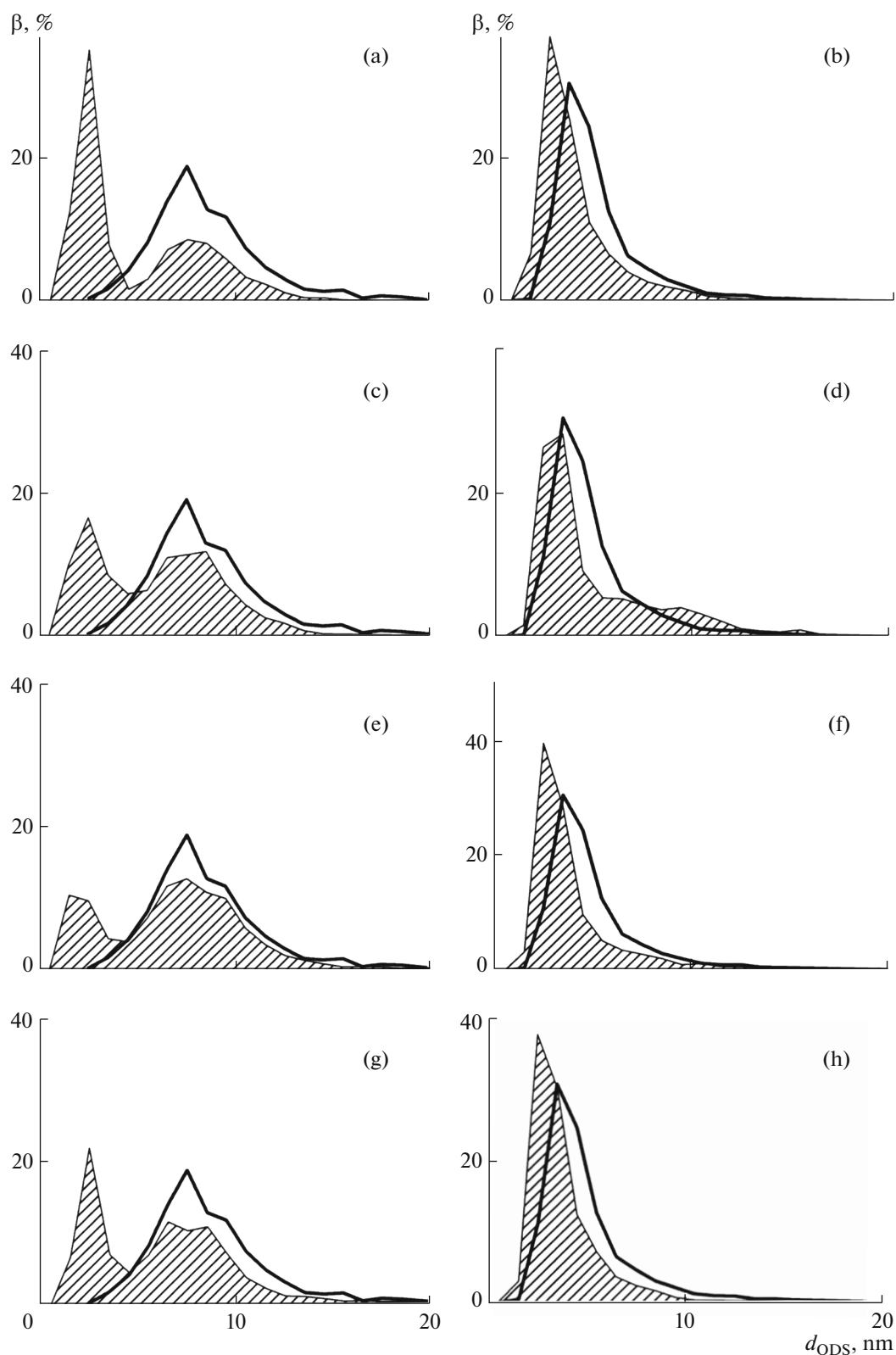


Fig. 4. Oxide particle size (d_{ODS}) distribution histograms in steels (a, c, e, g) ODS 13.5Cr, and (b, d, f, h) ODS 13.5Cr–0.3Ti in the initial state (solid thick lines) and after Ti^{2+} ion irradiation (thin lines) at (a, b) 300 K, (c–f) 573, and (g, h) 773 K to a fluence of (c, d) 10^{15} m^{-2} and (a, b, e–h) $3 \times 10^{15} \text{ cm}^{-2}$.

Table 2. TEM quantitative analysis of the oxide inclusions in the ion-irradiated ODS Eurofer and ODS 13.5Cr–(0–0.3)Ti steels in a FEI Tecnai F20 microscope

Steel	Type of ion	F, $\times 10^{15}$ ions/cm ²	D, dpa	T, K	\bar{d}_{ODS} , nm	N_{ODS} , $\times 10^{22}$ particles m ⁻³
ODS Eurofer	Fe ²⁺	1	0.9	300	5 ± 2	1.9
	Ti ²⁺	1	0.8	300	6 ± 3	1.6
ODS 13.5Cr	Fe ²⁺	1	0.9	300	12 ± 7*	0.4*
	Ti ²⁺	1	0.8	300	7 ± 5*	0.1*
		1	0.8	573	6 ± 3	1.9
		1	0.8	773	6 ± 3	1.7
		3	2.4	300	5 ± 3	3.2
		3	2.4	573	7 ± 3	1.3
ODS 13.5Cr–0.3Ti	Fe ²⁺	1	0.9	300	4 ± 2*	1.8*
	Ti ²⁺	1	0.8	300	6 ± 4*	0.4*
		1	0.8	573	4 ± 2	2.8
		1	0.8	773	4 ± 1	4.9
		3	2.4	300	4 ± 2	4.5
		3	2.4	573	4 ± 2	5.5

F is the fluence, D is the irradiation dose, \bar{d}_{ODS} is the average oxide size, and N_{ODS} is the number density of oxide particles.

* TEM data obtained on a JEOL JEM 1200EX microscope equipped with an LaB₆ cathode.

in the ODS 13.5Cr–0.3Ti steel irradiated up to doses of 0.8 and 2.4 dpa at 300 and 573 K. The titanium ion irradiation of the high-chromium ODS 13.5Cr steel at 300 and 573 K causes the formation of a new fraction of particles with an average size of 3 ± 1 nm. The observed changes in the size distribution of oxide inclusions can result from the rearrangement of the nanostructure (clusters and oxide particles) and the redistribution of chemical elements between the nanostructure constituents in the ODS steels during ion irradiation. However, the size distribution of oxide particles in the ODS 13.5Cr–0.3Ti steel in the initial state and after irradiation with Ti²⁺ ions up to a dose of 2.4 dpa at all chosen temperatures remains stable.

CONCLUSIONS

(1) The evolution of the nanostructure of the ODS Eurofer, ODS 13.5Cr, and ODS 13.5Cr–0.3Ti steels was studied after heavy-ion irradiation at 300, 573, and 773 K. These ODS steels were irradiated with Fe²⁺ (5.6 MeV) and Ti²⁺ (4.8 MeV) ions up to a fluence of 3×10^{15} cm⁻². It was found that a smaller number of dislocation loops formed in the material with an increased number of oxides. It is shown that irradiation reduced the average size of oxide particles, which could result from the cascade-induced dissolution of coarse oxides.

(2) The previously performed atom-probe tomography investigations, which revealed radiation-

induced changes in the chemical composition and the number density of nanoclusters in the ODS steels, suggest the redistribution of chemical elements between nanoclusters, matrix, and oxide particles. However, the size of oxide particles in the ODS 13.5Cr–0.3Ti and 13.5Cr steels after irradiation by 4.8-MeV Ti²⁺ ions at 573 and 773 K remains the same. This effect can be explained by the fact that the cascade dissolution of oxide particles is balanced by their growth due to the diffusion flux of atoms to the oxides at high temperatures.

ACKNOWLEDGMENTS

This work was partially supported by the Russian Foundation for Basic Research (project no. 13 02 91326 SIG a) and the Helmholtz–Russia Joint Research Group (project no. HRJRG-411).

REFERENCES

1. S. Ukai and M. Fujiwara, "Perspective of ODS alloys application in nuclear environments," J. Nucl. Mater. **307**, 749–767 (2002).
2. R. L. Klueh, P. J. Maziasz, I. S. Kim, L. Heatherly, D. T. Hoelzer, and N. Hashimoto, "Tensile and creep properties of an oxide dispersion strengthened ferritic steel," J. Nucl. Mater. **307–311**, 773–777 (2002).
3. R. Lindau, A. Möslang, M. Schirra, P. Schlossmacher, and M. Klimenkov, "Mechanical and microstructural properties of a hipped RAFM ODS-steel," J. Nucl. Mater. **307–311**, 769–772 (2002).

4. S. V. Rogozhkin, A. A. Aleev, A. G. Zaluzhnyi, A. A. Nikitin, N. A. Iskandarov, P. Vladimirov, R. Lindau, and A. Möslang, "Atom probe characterization of nanoscaled features in irradiated ODS Eurofer steel," *J. Nucl. Mater.* **409**, 94–99 (2011).
5. S. V. Rogozhkin, N. N. Orlov, A. A. Aleev, A. G. Zaluzhnyi, M. A. Kozodaev, R. P. Kuibeda, T. V. Kulevoy, A. A. Nikitin, B. B. Chalykh, R. Lindau, A. Möslang, and P. Vladimirov, "Nanostructure evolution in ODS eurofer steel under irradiation up to 32 dpa," *Phys. Met. Metallogr.* **116** (1), 72–78 (2015).
6. D. Brimbal, L. Beck, O. Troeber, E. Gaganidze, P. Trocellier, J. Aktaa, and R. Lindau, "Microstructural characterization of Eurofer-97 and Eurofer-ODS steels before and after multi-beam ion irradiation at JANNUS Saclay facility," *J. Nucl. Mater.* **465**, 236–244 (2015).
7. P. He, M. Klimenkov, R. Lindau, and A. Möslang, "Characterization of precipitates in nano structured 14% Cr ODS alloys for fusion application," *J. Nucl. Mater.* **428**, 131–138 (2012).
8. T. Kulevoy, R. Kuibeda, G. Kropachev, A. Kozlov, B. Chalyh, A. Aleev, A. Fertman, A. Nikitin, and S. Rogozhkin, "ITEP MEVVA ion beam for reactor material investigation," *Rev. Sci. Instr.* **81**, 02B906 (2010).
9. T. V. Kulevoy, B. B. Chalykh, P. A. Fedin, A. L. Sitnikov, A. V. Kozlov, R. P. Kuibeda, S. L. Andrianov, N. N. Orlov, K. S. Kravchuk, S. V. Rogozhkin, A. S. Useinov, E. M. Oks, A. A. Bogachev, A. A. Nikitin, N. A. Iskandarov, and A. A. Golubev, "Surface modification of ferritic steels using MEVVA and duoplasmatron ion sources," *Rev. Sci. Instr.* **87**, 02C102 (2016).
10. R. E. Stoller, M. B. Toloczko, G. S. Was, A. G. Certain, S. D. Dwaraknath, and F. A. Garner, "On the use of SRIM for computing radiation damage exposure," *Nucl. Instr. Met. Phys. Res. Sec. B* **310**, 75–80 (2013).
11. S. V. Rogozhkin, A. A. Bogachev, D. I. Kirillov, A. A. Nikitin, N. N. Orlov, A. A. Aleev, A. G. Zaluzhnyi, and M. A. Kozodaev, "Effect of alloying with titanium on the microstructure of an oxide dispersion strengthened 13.5% Cr steel," *Phys. Met. Metallogr.* **115** (12), 1259–1266 (2014).
12. M. Klimenkov, R. Lindau, and A. Möslang, "Direct correlation between morphology of $(\text{Fe,Cr})_{23}\text{C}_6$ precipitates and impact behavior of ODS steels," *J. Nucl. Mater.* **367–370**, 173–178 (2007).
13. M. Klimenkov, R. Lindau, and A. Möslang, "New insights into the structure of ODS particles in the ODS-Eurofer alloy," *J. Nucl. Mater.* **386–388**, 553–556 (2009).
14. A. Certain, S. Kuchibhatla, V. Shutthanandan, D. T. Hoelzer, and T. R. Allen, "Radiation stability of nanoclusters in nanostructured oxide dispersion strengthened (ODS) steels," *J. Nucl. Mater.* **434**, 311–321 (2013).

Translated by T. Gapontseva